

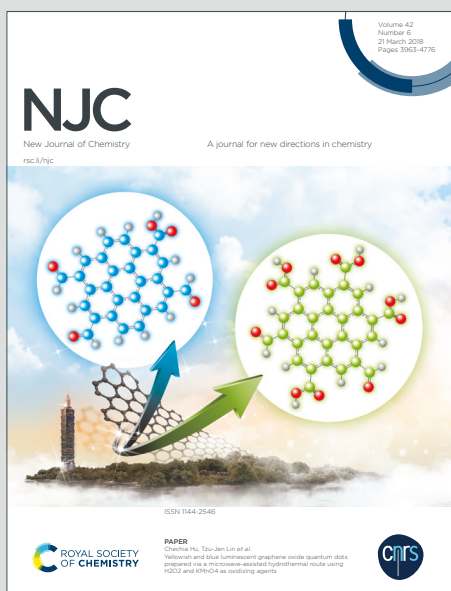
# NJC

New Journal of Chemistry

Accepted Manuscript

A journal for new directions in chemistry

This article can be cited before page numbers have been issued, to do this please use: M. Zhang, C. Wang, C. Zhang, T. Cai, L. Zhu and D. Xia, *New J. Chem.*, 2020, DOI: 10.1039/D0NJ01437K.



This is an Accepted Manuscript, which has been through the Royal Society of Chemistry peer review process and has been accepted for publication.

Accepted Manuscripts are published online shortly after acceptance, before technical editing, formatting and proof reading. Using this free service, authors can make their results available to the community, in citable form, before we publish the edited article. We will replace this Accepted Manuscript with the edited and formatted Advance Article as soon as it is available.

You can find more information about Accepted Manuscripts in the [Information for Authors](#).

Please note that technical editing may introduce minor changes to the text and/or graphics, which may alter content. The journal's standard [Terms & Conditions](#) and the [Ethical guidelines](#) still apply. In no event shall the Royal Society of Chemistry be held responsible for any errors or omissions in this Accepted Manuscript or any consequences arising from the use of any information it contains.

# Preparation and Catalytic Performance of a Novel Organometallic CoH/H $\beta$ catalyst for n-hexane isomerization

Mei Zhang <sup>a</sup>, Congcong Wang <sup>b</sup>, Chao Zhang <sup>a</sup>, Tingting Cai <sup>a</sup>, Lijun Zhu <sup>a,\*</sup> and Daohong Xia <sup>a,b,\*</sup>

<sup>a</sup> State Key Laboratory of Heavy Oil Processing, College of Chemical Engineering, China University of Petroleum (East China), Qingdao 266580, China,

<sup>b</sup> College of Chemical Engineering, Shengli College China University of Petroleum, Dongying 257061, China.

\* Corresponding author. E-mail: zhulijun@upc.edu.cn, xiadh@upc.edu.cn.

As a novel alkane isomerization catalyst, CoH/H $\beta$  was prepared by the reduction of CoH(P(OPh)<sub>3</sub>)<sub>4</sub>, which was pre-impregnated on the supporter of H $\beta$ . The prepared CoH/H $\beta$  catalyst was comparatively studied on the structures with CoH(P(OPh)<sub>3</sub>)<sub>4</sub>, CoH(P(OPh)<sub>3</sub>)<sub>4</sub>/H $\beta$  by FT-IR, TPR, SEM, XRD and other means. The results show that this new organometallic hydride catalyst was synthesized successfully and exhibited excellent catalytic performance for isomerization of n-hexane. For the best performance of CoH/H $\beta$  catalyst, the optimal catalytic reaction temperature, pressure, space velocity, and hydrogen/oil molar ratio were 300°C, 2.0 MPa, 1.0 h<sup>-1</sup>, and 4.0 in the isomerization process of n-hexane. Under the optimal reaction conditions, the conversion of n-hexane, the yield of isomerization, and the selectivity of iso-paraffins were 80.2 %, 63.0 %, and 78.6 %, respectively. This is mainly attributed to a new structure of Co-H hydride in CoH/H $\beta$  catalyst, which has strong hydrogenation/dehydrogenation activity in isomerization of n-hexane.

## 1. Introduction

Hydro-isomerization of n-alkanes have attracted much research attentions because of their high gasoline octane numbers and environmentally friendly properties.<sup>1-5</sup> Selectively isomerizing n-paraffins into iso-paraffins with catalysis, which can improve the octane number of a gasoline fraction, has been applied in industry.<sup>6-7</sup> For the isomerization catalysts, the aprotic acids were firstly applied for performing the isomerization of n-paraffins and it was difficult to meet industrial requirements owing to their low activity.<sup>8</sup> Then the noble metal bifunctional catalysts were systematically developed, which involved isomerization/cracking on acid sites and hydrogenation/dehydrogenation on metal sites. These industrial isomerization processes operated at high reaction pressure in general and had common drawbacks of high investment because of the presence of noble metals.<sup>1,9-13</sup>

So far, it's a great motivation to design new catalysts for the catalytic isomerization process. Non-noble metals such as Ni and Co are becoming new stars.<sup>14-18</sup> Jeong et al.<sup>14</sup> reported that the activity of Co, Ni, Fe, Mn, and Cu catalyst was measured in the hydrogenation reaction, and Co-catalyst exhibited a higher hydrogenation rate. Our previous investigation revealed that the performance of isomerization could be effectively promoted by introducing Ni-catalyst.<sup>19</sup> The non-noble metal catalyst seems to be a promising candidate as substitutes for traditional noble metals.

Transition metal hydrides have been widely used for various catalytic reactions, especially in the catalytic homogeneous isomerization of olefins, due to their unique structures, properties, and excellent chemical reactivity.<sup>20-24</sup> However, to our knowledge, there are no reports on the isomerization of n-hexane catalyzed by cobalt hydrides until now. Herein, a novel bifunctional Co-based transition metal hydride with unique structure was successfully synthesized and used in the isomerization of n-alkane for the first time. The preparation and reaction conditions for CoH/H $\beta$  in isomerization of n-hexane were studied to achieve the optimal catalytic performance and reaction mechanism.

## 2 Experiment section

### 2.1. Materials

Triphenyl phosphite (P(OPh)<sub>3</sub>, CP,  $\geq 99\%$ ), cobalt nitrate hexahydrate (Co(NO<sub>3</sub>)<sub>2</sub>·6H<sub>2</sub>O, AR,  $\geq 99\%$ ), ethanol

(C<sub>2</sub>H<sub>5</sub>OH, AR, ≥99%), sodium borohydride (NaBH<sub>4</sub>, AR, 96%), and xylene (C<sub>7</sub>H<sub>8</sub>, AR, 99%) were all provided by Sinopharm Chemical Reagent Co., Ltd. n-Hexane (C<sub>6</sub>H<sub>14</sub>, AR, ≥99%) and n-pentane (C<sub>5</sub>H<sub>12</sub>, AR, ≥99%) were purchased from Xilong Chemical Co., Ltd. Hβ molecular sieve was supplied by Tianjin Nanhua Catalyst Co., Ltd., with a specific surface area of 690 m<sup>2</sup>/g, silicon/aluminum atomic ratio of 25, crystallinity of more than 96.3% and particle size of 1.5 μm.

## 2.2. Preparation of Catalysts

CoH(P(OPh)<sub>3</sub>)<sub>4</sub> was synthesized according to the reported procedure.<sup>25</sup> P(OPh)<sub>3</sub> (3.1 g, 0.01 mol) was dissolved in a solution of Co(NO<sub>3</sub>)<sub>2</sub>·6H<sub>2</sub>O (0.582 g, 0.002 mol) in ethanol (20 mL). NaBH<sub>4</sub> (0.2 g, 0.005 mol), dissolving in hot ethanol (10 mL), was dropped into the stirred cobalt nitrate solution, and then it can be observed that the purple cobalt salt disappeared rapidly with a pale-yellow precipitate appeared. The precipitate was washed by ethanol and dried overnight at 80 °C in vacuum to give a pale-yellow crude product. The crude product was dissolved in hot xylene (50 mL), and filtered while hot and re-crystallized by adding ethanol to the filtrate. Then the final product CoH(P(OPh)<sub>3</sub>)<sub>4</sub> was obtained.

The purchased Hβ was disposed before the preparation of the catalyst precursor CoH(P(OPh)<sub>3</sub>)<sub>4</sub>/Hβ. At first, Hβ and Al<sub>2</sub>O<sub>3</sub> powder were uniformly mixed according to a certain mass ratio, and then added an appropriate amount of distilled water, and the composite was squeezed out from TBL-2 type catalyst forming device. The formed catalyst carrier was firstly baked under an infrared lamp, grinded to a certain particle size, and then activated in a muffle furnace at 300°C. The pretreated Hβ carrier was equal volume impregnation with a solution of CoH(P(OPh)<sub>3</sub>)<sub>4</sub> in dichloromethane for 24h, and dried at 80°C under N<sub>2</sub> for 2h. The obtained CoH(P(OPh)<sub>3</sub>)<sub>4</sub>/Hβ was further packed in the middle of a reaction tube, and reduced with hydrogen at 300°C for 3h. Finally, the catalyst CoH/Hβ was prepared.

## 2.3. Characterization of Catalysts and Catalytic Testing

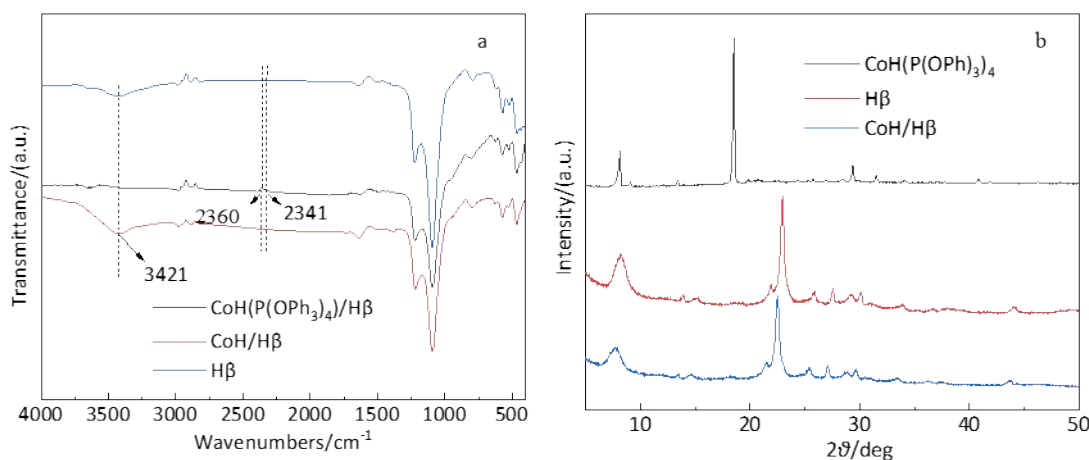
The synthesized catalysts were characterized by FT-IR, H<sub>2</sub>-TPR, NH<sub>3</sub>-TPD, SEM, XRD and other related means, and the catalyst performance was evaluated on a 550×8 mm fixed-bed reactor. For details, see supporting information S1 and S2.

## 3. Results and discussion

### 3.1. Characterization

Infrared spectra of P(OPh)<sub>3</sub>, CoH(P(OPh)<sub>3</sub>)<sub>4</sub>, CoH(P(OPh)<sub>3</sub>)<sub>4</sub>/Hβ, CoH/Hβ and Hβ were characterized to verify the existence of an unique structure of Co-H and listed in Fig. S1 and Fig.1a respectively.

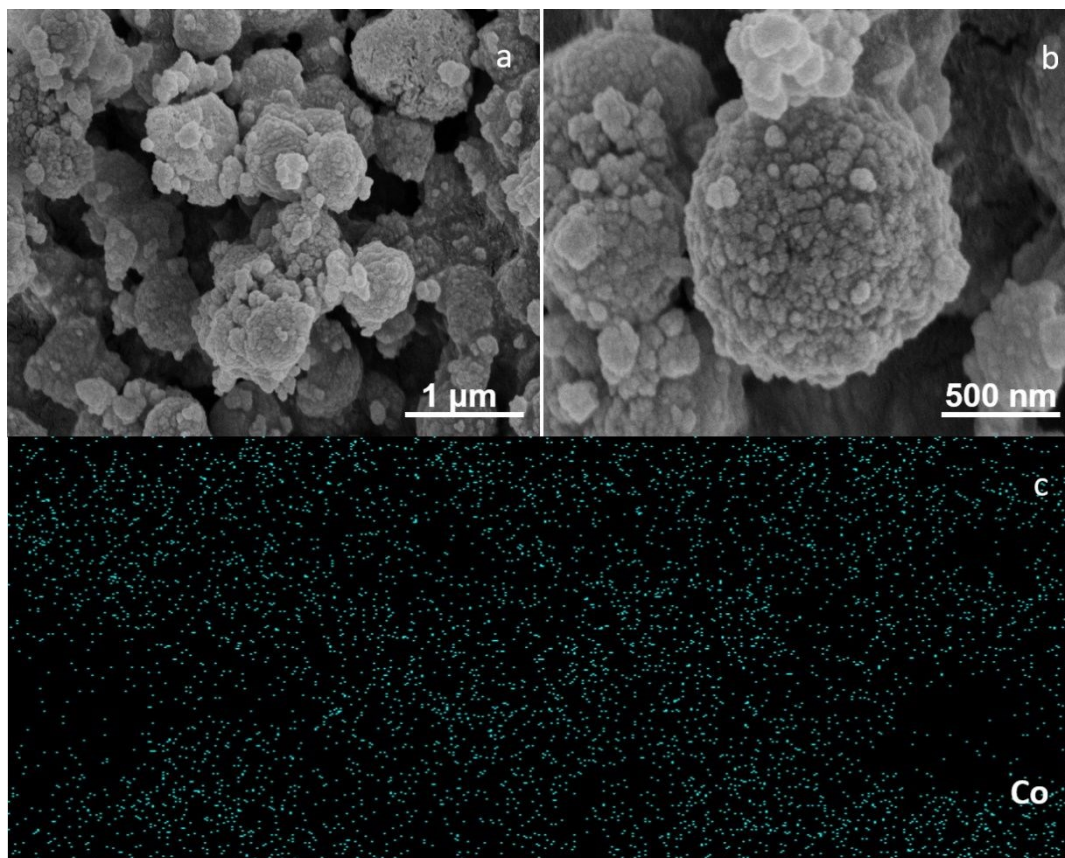
As shown in Fig. S1, two adjacent peaks of CoH(P(OPh)<sub>3</sub>)<sub>4</sub> at position of 2360 cm<sup>-1</sup> and 2345 cm<sup>-1</sup> respectively, appeared in its spectrum compared with that of P(OPh)<sub>3</sub>, which are ascribed to the stretching vibration of Co-P.<sup>26</sup> There was no obvious Co-H band of CoH(P(OPh)<sub>3</sub>)<sub>4</sub> could be observed in Fig. S1, because the vibration of Co-H bond very weak.<sup>27</sup> Fig. 1a shows that when CoH(P(OPh)<sub>3</sub>)<sub>4</sub> was loaded on disposed Hβ, its two characteristic peaks still existed in the spectrum while signal associated with the hydroxyl group of Hβ at band of 3421 cm<sup>-1</sup> doesn't emerge. Upon treatment of CoH(P(OPh)<sub>3</sub>)<sub>4</sub>/Hβ with hydrogen reduction at 300°C, the typical peaks of the obtained CoH/Hβ was similar with that of Hβ, demonstrating that the Co-P coordination bond disappeared, and novel catalyst CoH/Hβ equipped Co-H structure was obtained.



**Fig.1** FT-IR spectra of CoH(P(OPh)<sub>3</sub>)<sub>4</sub>/Hβ, CoH/Hβ and Hβ (a) and XRD patterns of CoH(P(OPh)<sub>3</sub>)<sub>4</sub>, the disposed Hβ and catalyst CoH/Hβ (b)

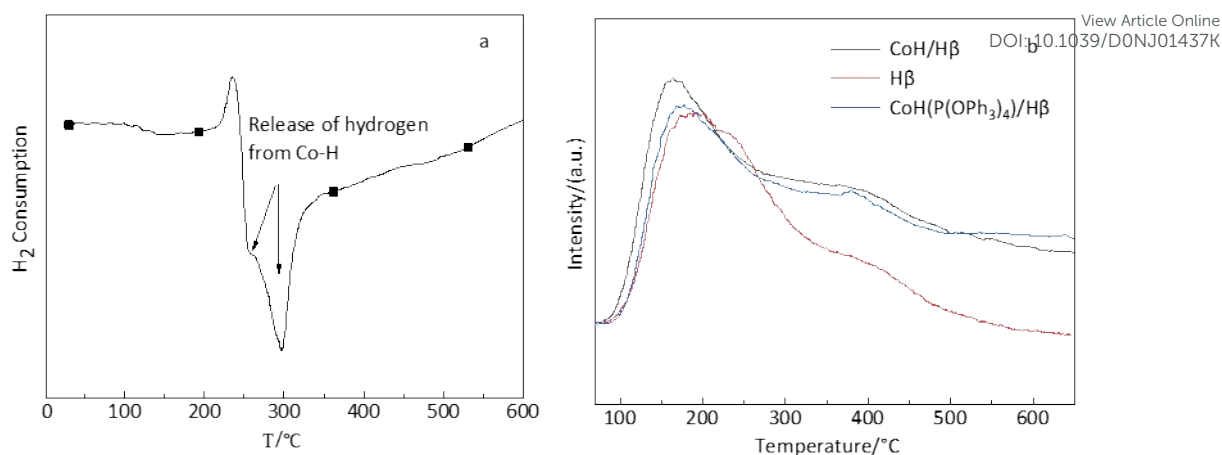
Fig. 1b lists the crystalline phase of CoH/H $\beta$ , the disposed H $\beta$  and the precursor CoH(P(OPh) $_3$ ) $_4$ . The diffraction peaks of CoH(P(OPh) $_3$ ) $_4$  are sharp and intense, indicating its highly crystallinity nature.<sup>28</sup> Interestingly, no obvious characteristic peaks assigned to CoH were detected after reduction, which implies the well-dispersion of CoH on H $\beta$ .

Fig. 2a and 2b show the SEM images of CoH/H $\beta$  at different scales and the element Co mapping was shown in Fig. 2c. It can be seen clearly from Fig. 2a and 2b that irregular spherical CoH nanoparticles were well dispersed on the surface of carrier, and the distribution of Co on H $\beta$  was uniform in Fig. 2c, which was consistent with the XRD results.



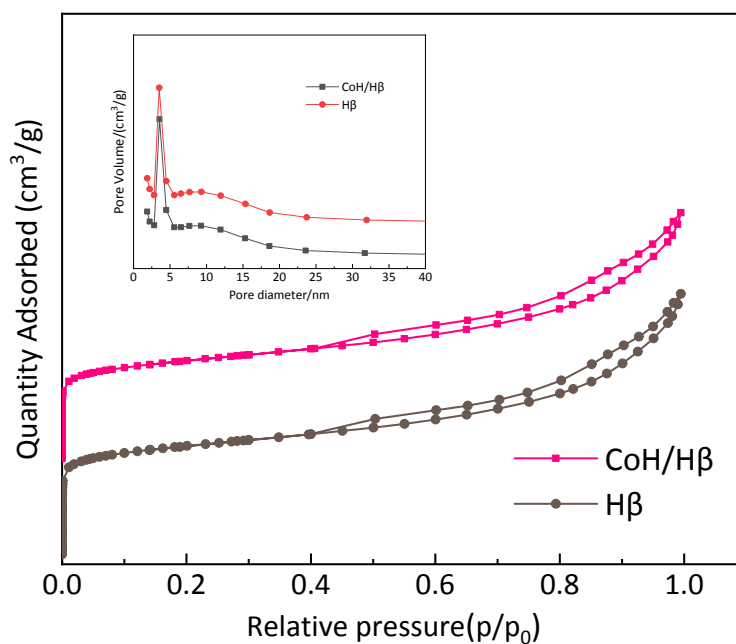
**Fig. 2** SEM images of CoH/H $\beta$  at different scales (a) 1 $\mu$ m, (b) 500 nm, and (c) Co mapping of CoH/H $\beta$ .

Fig. 3a exhibits the H $_2$  TPR curve of CoH(P(OPh) $_3$ ) $_4$ . There exists one reduction peak at 235 $^{\circ}$ C and another two adjacent negative peaks at 260 $^{\circ}$ C and 300 $^{\circ}$ C, respectively, indicating CoH(P(OPh) $_3$ ) $_4$  could be reduced at a temperature below 250 $^{\circ}$ C. The appearance of other two negative peaks, which is assumed to the disconnection of Co-H bond and the release of H $_2$  from CoH. The NH $_3$ -TPD Profiles of the disposed H $\beta$ , CoH(P(OPh) $_3$ ) $_4$ /H $\beta$  and CoH/H $\beta$  are presented in Figure 3b. The profiles of all samples show that there are two desorption peaks in the range of 100-600 $^{\circ}$ C and they are observed around 170 $^{\circ}$ C and 390 $^{\circ}$ C. The signal intensity of NH $_3$ -TPD profiles of CoH/H $\beta$  catalysts was stronger than that of CoH(P(OPh) $_3$ ) $_4$ /H $\beta$  and H $\beta$ , indicating that more weak and strong acid sites exist on CoH/H $\beta$  catalysts, especially the weak acid sites. The effect of carriers on n-hexane isomerization was shown in Fig. S4. As can be seen from Fig. S4, the conversion and yield of isomerization on H $\beta$  were higher than that of other two carriers.



**Fig. 3** H<sub>2</sub> TPR curve of CoH(P(OPh)<sub>3</sub>)<sub>4</sub> (a) and NH<sub>3</sub>-TPD profiles of CoH/Hβ, CoH(P(OPh)<sub>3</sub>)<sub>4</sub>/Hβ and the disposed Hβ (b).

Nitrogen adsorption isotherms were operated to verify the porous structure of catalyst CoH/Hβ and the disposed carrier Hβ, which are shown in Fig. 4. Both samples present the same isotherm types and have absorption at a relative pressure less than 0.2, which are characteristic of microporous materials.<sup>29</sup> With relative pressure ranges from 0.42 to 1.0, a significant absorption increase appears in Fig. 4, which means that the mesoporous structure may be formed by the accumulation of CoH particles over zeolite surface.<sup>30</sup> The mesopore sizes of CoH/Hβ and the disposed Hβ are concentrated between 2.5 nm and 7.5 nm, and pore size distribution (inset) is summarized in Fig. 4.



**Fig. 4** Nitrogen adsorption isotherms of CoH/Hβ and the disposed Hβ.

The pores structural characteristics of CoH/Hβ and the disposed Hβ based on nitrogen adsorption are encapsulated in Table 1.

**Table 1** Textural description of CoH/Hβ and the disposed Hβ.

Samples	$S_{\text{BET}}^a/\text{m}^2\cdot\text{g}^{-1}$	$V_{\text{mp}}^b/\text{cm}^3\cdot\text{g}^{-1}$	$V_{\text{T}}^c/\text{cm}^3\cdot\text{g}^{-1}$
CoH/Hβ	511.42	0.14	0.51

Disposed carrier H $\beta$ 

559.10

0.16

0.53

View Article Online  
DOI: 10.1039/D0NJ01437K<sup>a</sup> Specific surface area.  $S_{\text{BET}}$  was calculated by BET method.<sup>b</sup> Micropore volume.  $V_{\text{mp}}$  was calculated by t-plot method.<sup>c</sup> Total pore volume of samples.

Comparing with that of the disposed carrier H $\beta$ , the BET surface area of catalyst CoH/H $\beta$  decreased from 559.10 m<sup>2</sup>/g<sup>-1</sup> to 511.42 m<sup>2</sup>/g<sup>-1</sup>, and micropore volume reduced from 0.16 cm<sup>3</sup>/g<sup>-1</sup> to 0.14 cm<sup>3</sup>/g<sup>-1</sup>, indicating that the loading of active components only change the pore structure to a certain extent.

### 3.2. Effect of Preparation Conditions on the Catalytic Performance of CoH/H $\beta$

The preparation conditions, such as the activation temperature of catalyst, the loading of metal, and the particle size of carrier may have effects on the catalytic activity of the bi-functional catalyst CoH/H $\beta$ . In fact, the optimization of the preparation conditions, such as calcination temperature and heating rate, has been researched extensively.<sup>31-32</sup> The influence of preparation conditions of CoH/H $\beta$  on its catalytic behavior are shown in Fig. 5.

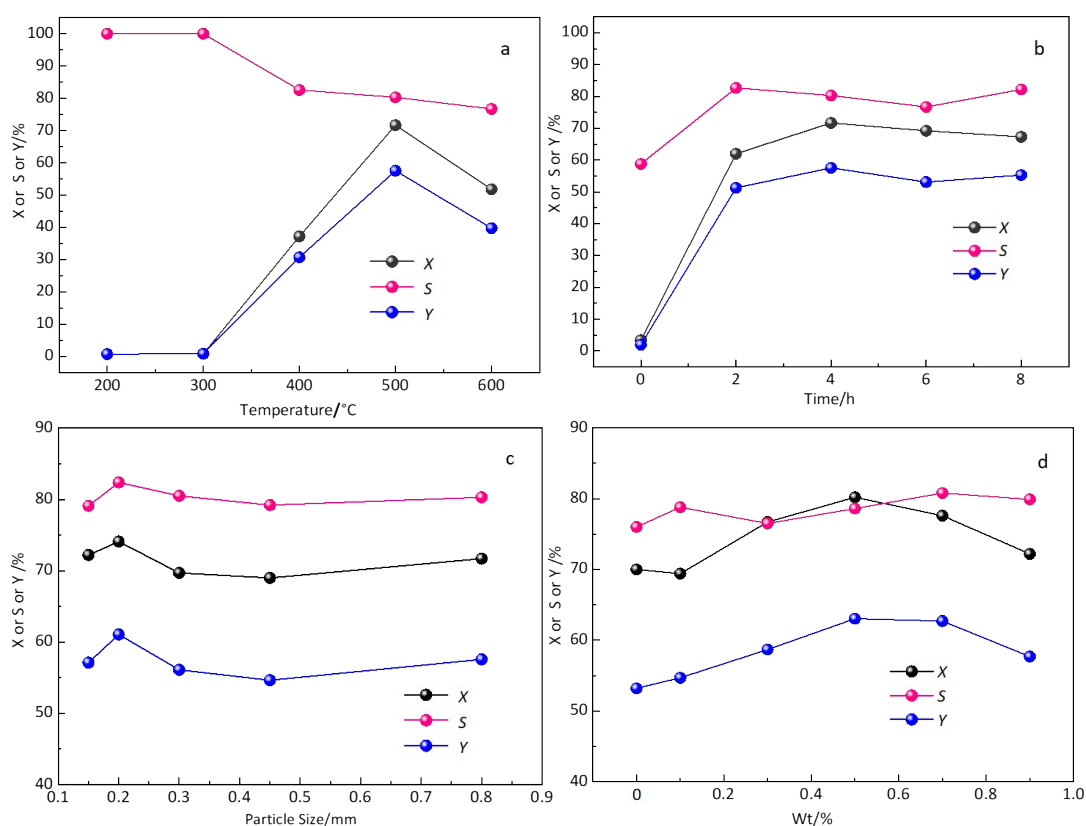


**Fig. 5** Effect of preparation conditions of CoH/H $\beta$  on n-hexane isomerization ( (a) activation temperature(activation time,4h; particle size, 0.2mm; Co loading in catalyst,0.5%), (b) activation time(activation temperature,500°C; particle size, 0.2mm; Co loading in catalyst,0.5%), (c) catalyst particle size(activation temperature,500°C; activation time,4h; Co loading in catalyst,0.5%) and (d) Co loading in catalyst (activation temperature,500°C; activation time,4h; particle size, 0.2mm;). )

Fig. 5a illustrates the effect of activation temperature on the catalytic behavior of CoH/H $\beta$  catalyst. The conversion and yield of isomerization both rise first when activation temperature was below 500°C, and then reach the maximum conversion rate (71.7%) and the maximum yield of isomer (57.6%) at 500°C. Then the conversion and yield of isomerization decrease with further increasing activation temperature, which was probably contributed to the destruction of the surface structure of CoH/H $\beta$  at high activation temperature.

Fig. 5b displays the influence of activation time on catalytic behavior of CoH/H $\beta$  catalyst. With the increase of activation time, the conversion of n-hexane, the selectivity of iso-paraffins, and the productivity of iso-paraffins rises flatly and then keeps in steady, respectively. A suitable activation time of CoH/H $\beta$  catalyst is 2 h.

The catalytic performance of CoH/H $\beta$  for n-hexane isomerization was found to be less dependent on particle

1  
2  
3 sizes of catalyst, as shown in Fig. 5c But it still showed a slight increase in isomerization when particle size of  
4 catalyst was 0.2 mm. Catalyst with small particle size has large surface area. However, catalyst with too smaller  
5 particle size results in dense catalyst bed, which leads to the pressure drop rise inside the reaction tube and the  
6 pipeline can potentially become blocked.

7  
8 Fig. 5d exhibits the effect of Co loading in CoH/H $\beta$  on the isomerization of n-hexane, showing the optimal  
9 catalytic activity was at 0.5wt.% of Co loading. iso-Hexane production decreased when Co loading on H $\beta$  was  
10 more than 0.5wt.%, which demonstrated that excessive Co loading may cause CoH particles to assemble over  
11 supporter surface and weak the catalytic performance of CoH/H $\beta$  catalyst.

### 12 3.3. Effect of Reaction Conditions on the Catalytic Performance of CoH/H $\beta$

13 The effects of different reaction conditions, such as reaction temperatures, pressures, hydrogen/oil molar ratios  
14 and mass space velocities, were investigated in order to obtain optimum catalytic performance of CoH/H $\beta$   
15 catalyst.

16 Fig. 6a shows the catalytic ability of CoH/H $\beta$  at different reaction temperatures for isomerization of n-hexane.  
17 As reaction temperature increases, the conversion of n-paraffin gradually increases, the selectivity of isomer  
18 declines. The yield of iso-hexane firstly elevates and then declines, and shows a maximum at 300°C. High  
19 temperature is benefit for the reaction kinetics of isomerization, but excessive heat leads to the side reaction like  
20 cracking. Therefore, 300°C seems to be a satisfactory reaction temperature to obtain high yield and selectivity for  
21 the entire isomerization reaction.

22 Fig. 6b displays the catalytic ability of CoH/H $\beta$  at different reaction pressures. As the reaction pressure  
23 increases from 1.0 MPa to 2.0 MPa, the yield and selectivity was increased, while the conversion was decreased.  
24 It was inferred, therefore, that an increasing in H<sub>2</sub> pressure promoted the hydrogenation of olefin intermediates  
25 generated during the isomerization process and inhibited the coking reaction of isomerization feeds. As H<sub>2</sub>  
26 pressure further increased from 2.0 MPa to 4.0 MPa, the yield of iso-hexane decreased, which was thought of  
27 high H<sub>2</sub> pressure preventing the dehydrogenation of n-hexane to olefins that was important to the isomerization  
28 process. Thinking about the feed conversion and the isomer yield, the H<sub>2</sub> pressure was optimized at 2.0 MPa.

29 The hydrogen oil molar ratio reflects the partial pressure of n-hexane in the gas phase of the reaction system.  
30 It's obviously in Fig. 6c that hydrogen to oil ratio with 4 is suitable. The lower ratio of hydrogen to oil is beneficial  
31 to the dehydrogenation of n-hexane to hexenes, which leads to high concentration of active olefins in the system  
32 and more isomerization reaction inducing. Conversely, high ratio of hydrogen to oil over normal range reduces  
33 the concentration of n-hexane in the gas phase and prevents the production of olefins.

34 Fig. 6d shows the influence of space velocities on catalytic behavior of CoH/H $\beta$ . The conversion of n-hexane  
35 reached 80.2% at the space velocity 1.0 h<sup>-1</sup>, while it decreased to 75% at 2 h<sup>-1</sup>. The change of yield of iso-hexane  
36 was similar, ranging from 63% at 1.0 h<sup>-1</sup> to 44 % at 2.5 h<sup>-1</sup>. These results could be explained by the fact that great  
37 space velocity shorted the residence time of n-hexane feedstock on the catalyst bed, leading to the inhibition of  
38 the isomerization of n-hexane. Therefore, mass space velocity 1.0 h<sup>-1</sup> was more suitable.

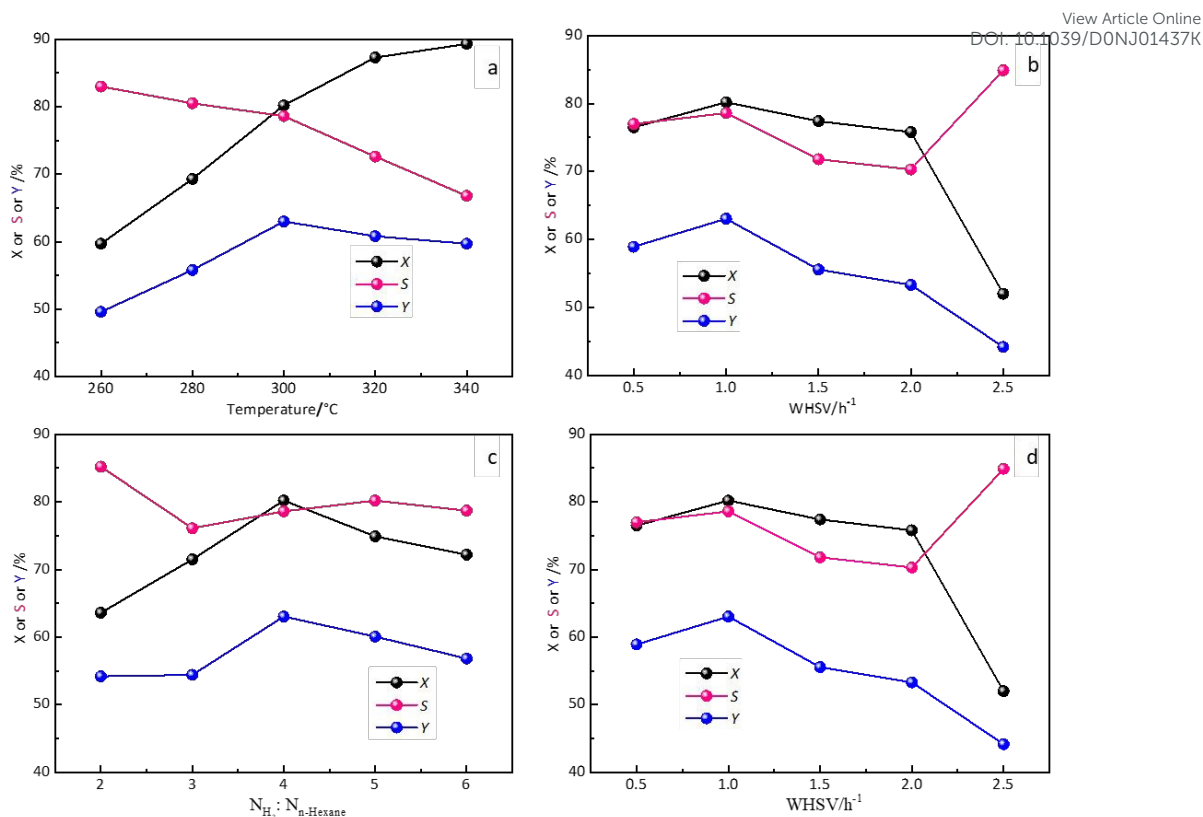


**Fig. 6** Effect of reaction conditions on n-hexane isomerization catalyzed by CoH/H $\beta$ . (a) reaction temperature (reaction pressure, 2.0MPa; WHSV, 1.0h<sup>-1</sup>; Hydrogen oil molar ratio, 4.0), (b) reaction pressure (reaction temperature, 300°C; WHSV, 1.0h<sup>-1</sup>; Hydrogen oil molar ratio, 4.0), (c) hydrogen to oil molar ratio (reaction temperature, 300°C; reaction pressure, 2.0MPa; WHSV, 1.0h<sup>-1</sup>), (d) mass airspeed (reaction pressure, 300°C; reaction pressure, 2.0MPa; Hydrogen oil molar ratio, 4.0).

### 3.4. Catalyst catalyzed isomerization of n-pentane and C<sub>5</sub>/C<sub>6</sub> mixed feedstock.

In order to further evaluate the catalytic performance of CoH/H $\beta$ , the isomerization of n-pentane and C<sub>5</sub>/C<sub>6</sub> mixed feedstock catalyzed by CoH/H $\beta$  were carried out respectively. Fig. S2 displays the effect of reaction temperature on n-pentane isomerization. The result is similar with that of the isomerization of n-hexane, which implies that temperature of 300°C is an optimum temperature for the isomerization reaction. The composition of C<sub>5</sub>/C<sub>6</sub> mixed feedstock influences the isomerization rate of light alkanes and the octane number of the obtained products, as shown in Table 2. Isomerization rates of alkanes and RON of products indicate the difference of depth of isomerization.

**Table 2.** The result of C<sub>5</sub>/C<sub>6</sub> mixed feedstock isomerization

Composition of C <sub>5</sub> /C <sub>6</sub> mixed feedstock (V <sub>n-C5</sub> /V <sub>n-C6</sub> )	C <sub>5</sub> isomerization rate /%	C <sub>6</sub> isomerization rate /%	RON
3:1	38.9	51.2	70.3
1:1	47.5	50.1	59.8
1:3	41.7	42.5	60.2

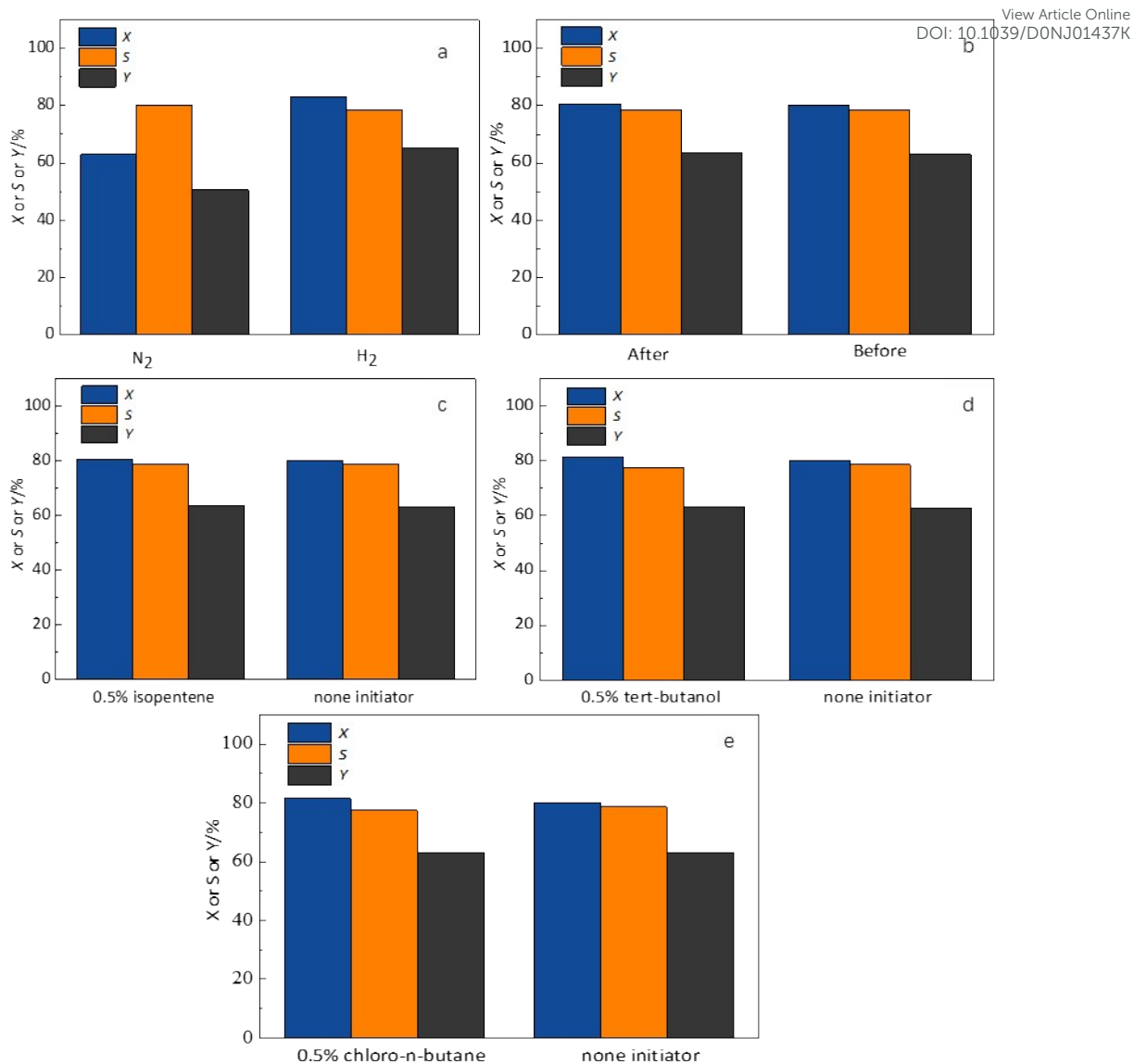
The C<sub>6</sub> isomerization rates are always higher than that of the C<sub>5</sub> feed in Table 2, which reveals n-hexane is easily isomerized than n-pentane. The reduction of RON of products becomes pronounced as the n-hexane increase in the C<sub>5</sub>/C<sub>6</sub> mixed feedstock.

### 3.5 Reaction mechanism

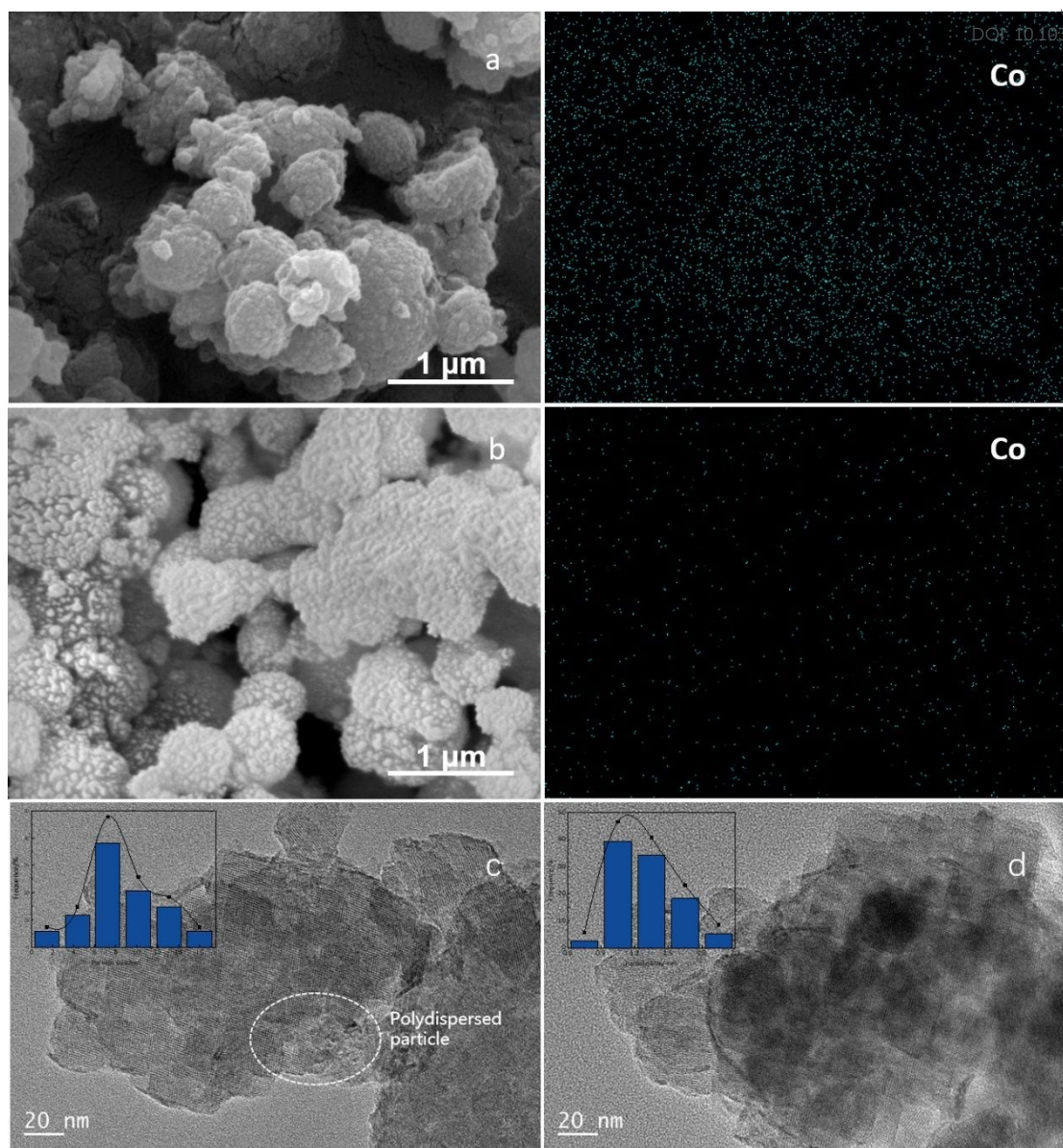
The mechanism for alkane isomerization catalyzed by traditional bifunctional catalysts is no longer a hot topic. However, the unique structure of cobalt hydride in the novel catalyst CoH/H $\beta$  may bring interesting information on the isomerization of n-paraffin. Firstly, the need for hydrogen was examined in the alkane isomerization with hydrogen and nitrogen atmosphere respectively.<sup>33</sup>

Fig. 7a shows that the catalytic performance of CoH/H $\beta$  in H<sub>2</sub> was better than that of in N<sub>2</sub>, which demonstrated hydrogen atmosphere was in favor of the isomerization. On the other hand, the catalytic performance of CoH/H $\beta$  before and after H<sub>2</sub> pre-reduction is almost same in Fig. 7b, indicating this novel catalyst doesn't require any H<sub>2</sub> pre-reduction operation, which provides a great advantage compared to traditional bifunctional catalyst. The study on the catalysts used in Fig. 7 has a definite assistance in proposing catalytic mechanisms. Therefore, XRD patterns of CoH/H $\beta$  before and after H<sub>2</sub> pre-reduction have been provided to study the change of the crystallinity and crystal phase in Fig. S3. It illustrated that characteristic peak intensity is of the same before and after H<sub>2</sub> pre-reduction. Meanwhile, the peak intensity significantly decreased after the catalyst used in N<sub>2</sub>. After further analyzing the SEM image and element Co mapping in SEM in Fig. 8a and 8b, the surface morphology of CoH/H $\beta$  did not change after H<sub>2</sub> reduction, and the distribution status of Co on H $\beta$  exhibits similar uniformity compared with catalyst before H<sub>2</sub> reduction in Fig. 2c. On the contrary, it emerged that carbon deposition covered on the catalyst surface of CoH/H $\beta$  after it was used in N<sub>2</sub> and the amount of Co element decreased clearly, this conclusion is in good agreement with the previous XRD analysis in Fig. S3.

In addition, TEM images with particle size charts of CoH/H $\beta$  were also studied in Fig. 8c and 8d. It can be seen from Fig.8c that the CoH particles was uniformly dispersed on the carrier, with the average particle size around 1.3 nm. While after the catalyst worked in N<sub>2</sub> (Fig.8d), the corresponding average particle sizes is closed to 9.3 nm, indicating obviously amorphous carbon covered on the catalyst surface and leading to reduce the catalytic performance. It turns out that isomerization reaction involves hydrogenation and dehydrogenation on the metal center of catalyst CoH/H $\beta$ , and the coking rate is delayed in H<sub>2</sub> atmosphere to maintain the activity of acid center.

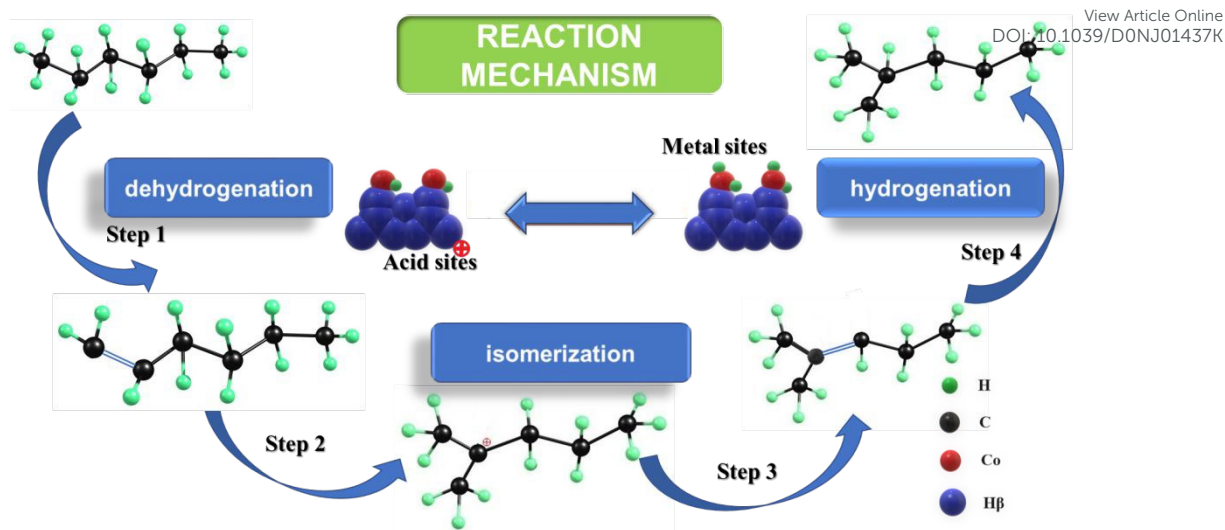


**Fig. 7** The effect of N<sub>2</sub> and H<sub>2</sub> on n-hexane isomerization (a), The effect of H<sub>2</sub> pre-reduction on the catalyst activity of CoH/H $\beta$  (b), The effect of isopentene (c), tert-butanol (d), and chloro-n-butane (e) on n-hexane isomerization (reaction temperature, 300°C; reaction pressure, 2.0 MPa; WHSV, 1.0 h<sup>-1</sup>; Hydrogen oil molar ratio, 4.0).



**Fig.8** SEM images and SEM mappings of CoH/H $\beta$  (a) H $_2$  pre-reduction for 2 h and (b) after worked in N $_2$ , TEM images with particle size charts of CoH/H $\beta$  (c) before and (d) after worked in N $_2$ .

The influence of several kinds of carbonium ions initiators (iso-pentene, tert-butanol, and chloro-n-butane) on catalytic behavior of CoH/H $\beta$  catalyst were then studied and the results are listed in Fig. 7c, 7d and 7e. In terms of these carbonium ions initiators, there was no obvious effect on catalytic isomerization, which demonstrated CoH/H $\beta$  catalyst itself having the function of catalytic producing carbonium ions. Therefore, alkane could be catalyzed to form olefin intermediate on metal sites of CoH/H $\beta$ , and then the intermediate converted to carbonium ions on acid sites of CoH/H $\beta$ , exhibiting synergetic properties in catalytic isomerization process<sup>34-35</sup>.



**Scheme 1** Mechanism of isomerization of n-hexane on CoH/Hβ

The reaction mechanism<sup>36-37</sup> includes four steps all together is proposed in scheme 1, which involves formation of n-hexene by dehydrogenation on CoH active center (Step 1), formation of n-C<sub>6</sub> carbonium ions over acid sites of zeolite (Step 2), transfer of n-C<sub>6</sub> carbonium ions into i-C<sub>6</sub> carbonium ions and formation i-C<sub>6</sub> hexene by deprotonation (Step 3), and finally hydrogenation of i-C<sub>6</sub> hexene to i-C<sub>6</sub> hexane over CoH/Hβ catalyst surface (Step 4). The good catalytic performance of CoH/Hβ was assumed to be the Co-H bond in the cobalt hydride that could be beneficial to hydrogenation and dehydrogenation in the isomerization process. The CoH metal sites worked together with the acid sites and synergically catalyzed the n-hexane isomerization.

## 4. Conclusion

In summary, the catalyst CoH/Hβ has been prepared successfully in this work through impregnation reduction method, which has not been reported up to now. The preparation and reaction conditions all have great influences on catalytic performance of the catalyst. Optimum catalysts activity and selectivity in the isomerization of n-hexane has been achieved at 300°C with a Co loading of 0.5 wt.%, in which the conversion of n-hexane, the selectivity of iso-paraffin and the yield of isomerization are 80.2%, 78.6% and 63.0%, respectively. The mechanism of isomerization of n-hexane on CoH/Hβ was investigated, which revealed that the synergetic catalytic action by acid and metal sites plays a key role in the performance of CoH/Hβ. The application of metal hydride loaded on zeolite will bring us some inspiration on the catalytic isomerization of light alkanes.

## Acknowledgments

This work was financially supported by the National Natural Science Foundation of China (Grant U1662115) and Shandong Province Natural Science Foundation (ZR2019MB057).

## References

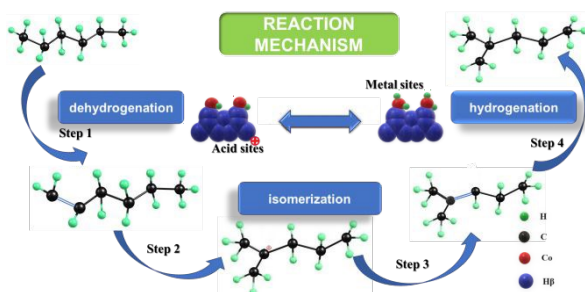
- 1 N. V. Chekantsev; M. S. Gyngazova; E. D. Ivanchina, *Chem. Eng. J.* 2014, 238, 120-128.
- 2 H. Ling; Q. Wang; B.-x. Shen, *Fuel Process. Technol.* 2009, 90, 531-535.
- 3 C. Zschiesche; D. Himsl; R. Rakoczy; A. Reitzmann; J. Freiding; N. Wilde; R. Gläser, *Chem. Ing. Tech.* 2017, 89, 956-962.
- 4 L. Ge; G. Yu; X. Chen; W. Li; W. Xue; M. Qiu; Y. Sun, *New J. Chem.* 2020, 44, 2996-3003.
- 5 T. Pinto; P. Arquilliere; G. P. Niccolai; F. Lefebvre; V. Dufaud, *New J. Chem.* 2015, 39, 5300-5308.
- 6 V. M. Akhmedov; S. H. Al-Khowaiter, *Catalysis Reviews* 2007, 49, 33-139.
- 7 Y. Lyu; Y. Liu; L. Xu; X. Zhao; Z. Liu; X. Liu; Z. Yan, *Appl. Surf. Sci.* 2017, 401, 57-64.
- 8 I. Akhrem; S. Gudima; M. Vol'Pin, *Chemistry A European Journal* 1996, 2, 812-814.
- 9 K. Arata; H. Matsushashi; M. Hino; H. Nakamura, *Catal. Today* 2003, 81, 17-30.
- 10 J. E. Samad; J. Blanchard; C. Sayag; C. Louis; J. R. Regalbutto, *J. Catal.* 2016, 342, 203-212.
- 11 T. Matsuda; H. Sakagami; N. Takahashi, *Catal. Today* 2003, 81, 31-42.
- 12 Q. Ning; H. Zhang; Y. He; Z. Chen; J. Ren, *New J. Chem.* 2019, 43, 13967-13978.

- 1  
2  
3 13 X. Wu; Minghuang Qiu; Xinqing Chen; Gan Yu; Xing Yu; Chengguang Yang; Jian Sun; Ziyu Liu; New Article Online  
DOI: 10.1039/D0NJ01437K  
4 Yuhan Sun, *New J. Chem.* 2018, 42, 111-117.
- 5 14 S. U. Jeong; R. K. Kim; E. A. Cho; H. J. Kim; S. W. Nam; I. H. Oh; S. A. Hong; S. H. Kim, *J. Power*  
6 *Sources* 2005, 144, 129-134.
- 7 15 J.S. Chen; T. Cai; X. Jing; L. Zhu; Y. Zhou; Y. Xiang; D. Xia, *Appl. Surf. Sci.* 2016, 390, 157-166.
- 8 16 A. Masalska; J. R. Grzechowiak; K. Jaroszevska, *Top. Catal.* 2013, 56, 981-994.
- 9 17 P. M. Lima; T. Garetto; C. L. Cavalcante; D. Cardoso, *Catal. Today* 2011, 172, 195-202.
- 10 18 G. Xing; S. Liu; Q. Guan; W. Li, *Catal. Today* 2019, 330, 109-116.
- 11 19 J. Chen; Z. Duan; Z. Song; L. Zhu; Y. Zhou; Y. Xiang; D. Xia, *Appl. Surf. Sci.* 2017, 425, 448-460.
- 12 20 R. Uma; C. Crévisy; R. Grée, *Chem. Rev.* 2003, 103, 27-52.
- 13 21 T. Shima; Z. Hou, Dinitrogen Fixation by Transition Metal Hydride Complexes. In *Nitrogen Fixation*,  
14 Nishibayashi, Y., Ed. 2017; Vol. 60, pp 23-43.
- 15 22 M. A. A.-O. Hany M. AbdelDayem, *Ind. Eng. Chem. Res.* 2008, 47, 1011-1016.
- 16 23 K. M. Waldie; F. M. Brunner; C. P. Kubiak, *ACS Sustainable Chemistry & Engineering* 2018, 6, 6841-  
17 6848.
- 18 24 W. K. Hu; D. Noréus, *Electrochem. Commun.* 2009, 11, 2212-2215.
- 19 25 J. J. Levison; S. D. Robinson, *Inorg. Synth.* 1972, VIII, 105-112.
- 20 26 D. M. L. Goodgame; A. M. Z. Slawin; D. J. Williams, *Polyhedron* 1987, 6, 543-547.
- 21 27 H. Liu; X. Meng; R. Zhang; Z. Liu; J. Meng; C. Xu, *Catal. Commun.* 2010, 12, 180-183.
- 22 28 D.H. Xia; T.T. Cai; L.J. Zhu; S.J. Jiang; Z.B. Duan; Linbin Yang, *ACTA PETROLEI SINICA(PETROLEUM*  
23 *PROCESSING SECTION)* 2019, 35, 40-48.
- 24 29 J. Chen; T. Cai; X. Jing; L. Zhu; D. Xia, *Appl. Surf. Sci.* 2016, 390, 157-166.
- 25 30 S. Triwahyono; A. A. Jalil; N. N. Ruslan; H. D. Setiabudi; N. H. N. Kamarudin, *J. Catal.* 2013, 303,  
26 50-59.
- 27 31 J. de Graaf; A. J. van Dillen; K. P. de Jong; D. C. Koningsberger, *J. Catal.* 2001, 203, 307-321.
- 28 32 C. H. Wu; Q. R. Zhao; J. Y. Zhang; D. D. Zhu; G. B. Du, *Advanced Materials Research* 2011, 295-  
29 297, 156-160.
- 30 33 C. Bouchy; G. Hastoy; E. Guillon; J. A. Martens, *Oil & Gas Science and Technology - Revue de l'IFP*  
31 2009, 64, 91-112.
- 32 34 X. R. Chen; Y. Q. Du; C.L. Chen; N.P. Xu; C.Y. Mou, *Catal. Lett.* 2006, 111, 187-193.
- 33 35 Y. Guan; B. Yang; S. Qi; C. Yi, *Ind. Eng. Chem. Res.* 2011, 50, 9054-9062.
- 34 36 J. Macht; R.T. Carr; E. Iglesia, *J. Am. Chem. Soc.*, 2009, 131, 6554-6565.
- 35 37 F.J.M.M. Gauw; J. Grondelle; R.A. Santen, *J. Catal.*, 2002, 206, 295-304.
- 36  
37  
38  
39  
40  
41  
42  
43  
44  
45  
46  
47  
48  
49  
50  
51  
52  
53  
54  
55  
56  
57  
58  
59  
60

## Preparation and Catalytic Performance of a Novel Organometallic CoH/H $\beta$ catalyst for n-hexane isomerization

View Article Online  
DOI: 10.1039/C9/DONJ01437K

A novel organometallic catalyst CoH/H $\beta$  was synthesized and directly provide hydrogenation/dehydrogenation effects in isomerization of n-hexane



1  
2  
3  
4  
5  
6  
7  
8  
9  
10  
11  
12  
13  
14  
15  
16  
17  
18  
19  
20  
21  
22  
23  
24  
25  
26  
27  
28  
29  
30  
31  
32  
33  
34  
35  
36  
37  
38  
39  
40  
41  
42  
43  
44  
45  
46  
47  
48  
49  
50  
51  
52  
53  
54  
55  
56  
57  
58  
59  
60